Electronic Supplementary Information

Tumor Chemical Suffocation Therapy by Dual Respiratory Inhibitions

Yingying Xu,[a,b] Yuedong Guo,[a] Lei Chen,[c] Dalong Ni,[a] Ping Hu,*[a] and Jianlin Shi*[a,d]

[a.] The State Key Laboratory of High Performance Ceramics and Superfine Microstructures, Shanghai Institute of Ceramics, Chinese Academy of Sciences, 1295 Ding-xi Road, Shanghai 200050, P.R. China.

[b.] School of Physical Science and Technology, ShanghaiTech University, 393 Middle Hua-xia Road, Shanghai 201210, P.R. China.

[c.] Department of Chemistry, Fudan University, 220 Han-dan Road, Shanghai 200433, P.R. China.

[d.] Innovative Center of Medicine, Shanghai Tenth People□s Hospital, 38 Yun-xin Road, Shanghai 200435, P.R. China.

Correspondence to: jlshi@mail.sic.ac.cn (J. Shi); huping@mail.sic.ac.cn (P. Hu)

Contents

Section A: Experimental Details

Synthesis of mesoporous silica nanoparticles (MSNs). MSNs were synthesized *via* the procedure mentioned in the literature.[1] Firstly, 20 mL solution containing hexadecyl trimethyl ammonium chloride (CTAC, 2 g) and triethanolamine (TEA, 0.08 g) was added to a 60 mL jar, and then the mixture was heated to 95 °C under intensive stirring for 1 h. Then tetraethyl orthosilicate (TEOS, 1.5 mL) was dropwise added into the reaction system and stirred for another hour. The products were collected by centrifugation at the rate of 20000 r/min for 15 min and washed using ethanol for three times in order to remove the residual reactants. Afterward, MSNs were extracted with 60 mL of sodium chloride (NaCl) in methanol solution (1 wt%) to remove CTAC at room temperature for 3 h. The resulting MSNs were obtained by centrifugation and drying in a lyophilizer.

Fabrication of NH_2-modified mesoporous silica nanoparticles (MSNs-NH_2). The surface of MSNs was modified with amino groups *via* the treatment of APTES. MSNs (25 mg) were first dispersed in ethanol (25 mL), and then the solution was refluxed at 78 °C for 6 h, followed by the addition of APTES (50 μL). After centrifugation (20000 r/min, 15 min) and washed with water for 3 times, MSNs-NH_2 were redispersed in water (25 mL).

Preparation of PAASH. PAASH was prepared according to the method used in the literature.[2] 1-ethyl-3-(3-dimethly-aminopropyl) carbodiimide (EDC, 70 mg) and Poly(acrylic acid) (PAA, 250 mg) were dissolved in turn in the 5 mL of phosphate buffer solution (0.1 M, pH 7.4). Then N-hydroxysuccinimide (NHS, 45 mg) was added to the solution and the mixture was magnetically stirred at the speed of 600 r/min for 15 min. The reaction system was stirred for 24 h at room temperature, followed by dissolving cysteamine hydrochloride (7.5 mg) in the solution. After the mixture was dialyzed vigorously against deionized water for 24 h, the products were obtained by freeze-drying. The resulting polymer was further purified through precipitation from water into dioxane. PAASH (10 mg/mL) was incubated in a solution of DTT (100 mg/mL) in PBS (10 mM, pH 8) for over 12 h at room temperature to separate the polymer chains.

Synthesis of MP nanoparticles. MSNs-NH_2 (20 mg) were stirred in PVP (1 mg/mL, 5 mL) solution and PAASH solution (1 mg/mL, 5 mL) successively both for 10 min. Finally, MPER nanoparticles were obtained by crosslinking the thiols in a 10 mL of solution of chloramine T (2 mM) in MES (50 mM, pH 6) for 90 s at room temperature.

Synthesis of MPE nanoparticles. MSNs-NH_2 (20 mg) were first dispersed in water (5 mL), and EDTA (80 mg) were added into mixture. The mixture was magnetically at room temperature for 24 h. After centrifugation, MSNs-NH_2 were stirred in PVP (1 mg/mL, 5 mL) solution and PAASH solution (1 mg/mL, 5 mL) successively both for 10 min. Finally, the MPER nanoparticles were obtained by crosslinking the thiols in a 10 mL of solution of chloramine T (2 mM) in MES (50 mM, pH 6) for 90 s at room temperature.

Synthesis of MPR nanoparticles. MSNs-NH_2 (20 mg) was first dispersed in water (5 mL), and Rotenone/DMSO solution (1 mg/mL) were added into mixture. The mixture was magnetically at room temperature for 24 h. After centrifugation, MSNs-NH_2 were stirred in PVP (1 mg/mL, 5 mL) solution and PAASH solution (1 mg/mL, 5mL) successively both for 10 min. Finally, the MPER nanoparticles were obtained by crosslinking the thiols in a 10 mL of solution of chloramine T (2 mM) in MES (50 mM, pH 6) for 90 s at room temperature.

Synthesis of MPER nanoparticles. MSNs-NH_2 (20 mg) was first dispersed in water (5 mL), and then Rotenone/DMSO solution (1 mg/mL) and EDTA (80 mg) were added into mixture. The mixture was magnetically at room temperature for 24 h. After centrifugation, MSNs-NH_2 were stirred in PVP (1 mg/mL, 5 mL) solution and PAASH solution (1 mg/mL, 5mL) successively both for 10 min. Finally, the MPER nanoparticles were obtained by crosslinking the thiols in a 10 mL of solution of chloramine T (2 mM) in MES (50 mM, pH 6) for 90 s at room temperature.

Characterization. Transmission electron microscopy (TEM) images were acquired with a JEM-2100F electron microscope at 200 kV. Scanning transmission electron microscopy (STEM) images, corresponding element mapping and EDS spectrum were obtained with FEI Magellen at 5 kV. The zeta potential and size distribution were conducted on Zetasizer Nanoseries (Nano ZS90). Fourier transform infrared spectroscopy (FT-IR) spectra were recorded on a Nicolet 7000-C spectrometer. Nitrogen adsorption-desorption isotherms at 77 K were measured on a Micrometitics Tristar 3000 system. UV-vis-NIR absorption spectra were determined by UV-3600 Shimadzu UV-vis-NIR spectrometer with QS-grade quartz cuvettes. The element concentration was recorded by Agilent 700 Series inductively coupled plasma optical emission spectrometry (ICP-OES). TGA pattern was measured by Rigaku's Thermoplus EVO II thermal analyzer. Confocal laser-scanning microscope (CLSM) images were acquired on an FV1000 CLSM. Flow cytometric analyses were obtained on a BD LSRFortessa flow cytometer.

The releasing profiles of MPER. 30 mg MPER nanoparticles were sealed in a dialysis tube (3.5 kda) and dispersed in PBS (15 mL). the releasing profiles were performed in a shaking table at 37 °C and at the speed of 150 rpm. The EDTA releasing profile was obtained by fluorescence spectrometer and Rotenone releasing profile was obtained by UV-vis. Briefly, 100 μL of 10^{-3} M/L SSA solution was mixture with 100, 80, 60, 40, 20,10, 5 and 0 μL of 10^{-3} M/L Fe^{3+}. Then the mixture was diluted to 5 mL using acetate buffer (pH = 3.8). After shaking at 150 rpm and 25 °C for 30 minutes, the mixture was measured by fluorescence spectrometer. Then the linear curve of Fe^{3+} concentration and SSA fluorescence intensity can be obtained. 20 μL of liquid extracted in PBS at different moments was mixed with 100 μL of 10^{-3} M/L SSA and was further diluted to 5 mL of acetate buffer. The fluorescence intensity of the mixture was detected by fluorescence spectrometer.

As for the Rotenone releasing profile was obtained by UV-vis. 30 mg MPER nanoparticles were sealed in a dialysis tube (3.5 kda) and dispersed in PBS/DMSO (15 mL). 3 mL of above-mentioned solution was measured by UV-vis at specific time. The maximal adsorption of wavelength is at 290 nm.

Intracellular endocytosis in 4T1 cells by CLSM observation. For CLSM observations, 4T1 cells (1×10^5 cells per dish) were planted in coverglass bottom dishes (35 mm × 10 mm, Corning Inc., USA), and then treated with nanoparticles at the same final concentration of 200 μg/mL. After the incubation for different time periods (1 h, 4 h and 8 h), the media in the dishes were removed, and then the cells were washed twice with PBS in order to remove the residual nanoparticles. Then, 0.5 mL of DAPI (4, 6-diamidino-2-phenylindole)/methanol solution (V/V_0 = 10%) was added into the dishes. Next, the cells were incubated for 10 min to stain the nuclei. After the incubation, the 4T1 cells were softly washed with methanol for three times in order to remove excessive DAPI. Finally, 1mL of PBS (pH = 7.4) was added and the 4T1 cells were visualized using a confocal laser scanning microscope (FluoView FV1000, Olympus). The fluorescence images were obtained under 60× oil-immersion objective. Green and blue luminescent emissions from FITC and DAPI were excited at 488 nm and 405 nm, respectively. The emission wavelengths of FITC and DAPI were ranged from 500 nm to 550 nm and from 425 nm to 475 nm, respectively.

Flow cytometric fluorescence intensity analysis and CLSM images of intracellular Mg^{2+}. The 4T1 cells were cultured with DMEM culture medium (GIBCO, USA) with 10% fetal bovine serum (GIBCO, USA). All cells were cultured in a humidified incubator (5% CO_2) at 37 °C. For flow cytometric analysis, the 4T1 cells were planted into a 6-well plate (2×10^5 per well) and allowed to adhere for 24 h. Then 4T1 cells were incubated with MPE nanoparticles (800, 400, 200 and 0 μg/mL) for 24 h. The intracellular Mg^{2+} variations were tested *via* the indicator Mag-Fura-4 AM (US EVERBRIGHT. Inc) according to the manufacturer's instructions. First, 4T1 cells were preincubated in physiological medium with 120 mM NaCl, 20 mM HEPES, 4.7 mM KCl, 1.2 mM KH_2PO_4, 1.2 mM $MgSO_4$, 1.25 mM $CaCl_2$, and 10 mM glucose at temperature 37 °C for 10 min to allow stabilization and equilibration of ion gradients. Then the prepared indicator solution of Mag-Fura-4 AM (1 mM) was dispersed in anhydrous DMSO. Next, a dispersion of the AM ester was prepared by vigorously mixing 4 μL of indicator solution and 5 μL of 20% (w/v) Pluronic F-127 (Sigma, USA) in 1 mL of medium. Afterward, the final concentration for the indictor (1 μM) was obtained by adding 0.25 mL of this dispersion per 0.75 mL of cell containing medium. Then, incubated for another 30 min, the cells were washed for three times in the final incubation medium and then incubated for 30 min to allow complete de-esterification of intracellular AM esters. The fluorescence intensity of cells was measured by flow cytometry (BD, USA) (λ_{ex} = 480 nm, λ_{em} = 520 nm).

The HUVECs were cultured with 1640 culture medium (UBI, Shanghai) with 10% fetal bovine serum (UBI, Shanghai). All cells were cultured in a humidified incubator (5% CO_2) at 37 °C. For flow cytometric analysis, the 4T1 cells were planted into a 6-well plate (2×10^5 per well) and allowed to adhere for 24 h. Then 4T1 cells were incubated with MPE nanoparticles (800, 400, 200, 100 and 0 μg/mL) for 24 h. The intracellular Mg^{2+} variations were tested *via* the indicator Mag-Fura-4 AM (Shanghai Maokang Biotechnology. Inc) according to the manufacturer's instructions. The cells were incubated in the 1640 culture medium containing 1 μM of Mag-Fura-4 AM for 60 min. After medium was removed, the cells were washed with HBSS for 3 times

and then incubated with HBSS for another 30 minutes. The fluorescence intensity of cells was measured by flow cytometry.

Fluorescence intensity analysis of intracellular Ca^{2+} by flow cytometric analysis. The 4T1 cells were cultured with DMEM culture medium (GIBCO, USA) with 10% fetal bovine serum (GIBCO, USA). All cells were cultured in a humidified incubator (5% CO_2) at 37 °C. For flow cytometric analysis, the 4T1 cells were planted into a 6-well plate (2×10^5 per well) and allowed to adhere for 24 h. Then 4T1 cells were incubated with MPE nanoparticles (400 and 0 μg/mL) for 24 h. The intracellular Ca^{2+} variations were tested *via* the indicator Fluo-4 AM (Beyotime Institute of Biotechnology, Jiangsu, China) according to the manufacturer's instructions. After removing the medium, we washed 4T1 cells with PBS for 3 times. Then 0.5 μM Fluo-4 AM probe was incubated with cells for 25 minutes. Next, the cells were cultured for another 24 hours after the probe was removed. The fluorescence intensity of intracellular Ca^{2+} was analysed by flow cytometric analysis.

Detection of hexokinase activity, phosphofructokinase activity and pyruvate kinase activity. The 4T1 cells were seeded in 6-well plates at a density of 10^5 cells per well and cultured in 5% CO_2 at 37 °C for 24 h to allow the cells to attach. Then the cells were treated with 400 μg/mL MPE nanoparticles for another 24 h or 48 h. At last, the cells were washed three times by PBS. The intracellular Hexokinase activity was obtained by the protocol of the Hexokinase assay kit (Nanjing Jiancheng Bioengineering Institute, Nanjing, China). The intracellular Hexokinase activity was obtained by the protocol of the Phosphofructokinase assay kit (Nanjing Jiancheng Bioengineering Institute, Nanjing, China). The intracellular Pyruvate Kinase activity was obtained by the protocol of the Phosphofructokinase assay kit (Nanjing Jiancheng Bioengineering Institute, Nanjing, China).

Detection of ATP concentration. The ATP concentration of 4T1 cells after being incubated with various dosages of MPE or MPER nanoparticles. The 4T1 cells were seeded in a culture dish (Corning Inc., USA) at a density of 10^7 cells per well and then cultured at 37 °C in 5% CO_2 for at least 12 h to allow the cells to attach. Then the cells were treated with 100, 200 and 400 μg/mL MPE or MPER nanoparticles for another 24 h. At last, the cells were washed three times by PBS. The intracellular ATP concentration was obtained by the protocol of the ATP assay kit (Beyotime Institute of Biotechnology, Jiangsu, China).

The ATP concentration of 4T1 cells after incubation with Fluo-4 AM (Beyotime Institute of Biotechnology, Jiangsu, China). The 4T1 cells were seeded in a culture dish (Corning Inc., USA) at a density of 10^7 cells per well and then cultured at 37 °C in 5% CO_2 for at least 12 h to allow the cells to attach. After the culture was removed, the 4T1 cells were washed by PBS for 3 times. Then the cells were incubated with Fluo-4 AM (0.5 μM, diluted by PBS) for 25 minutes. Next, the cells were incubated with the culture media for another 24 h. The intracellular ATP concentration was measured by the protocol of the ATP assay kit (Beyotime Institute of Biotechnology, Jiangsu, China).

Mitochondrial morphology by Bio-TEM observation. The 4T1 cells were incubated with 0 and 400 μg/mL of nanoparticles and 10 μg/mL free Rotenone for 24

h. The cells were then washed with PBS for three times and detached by being incubated with 0.25% trypsin for 5 min. Next, the 4T1 cells suspension was centrifuged at 1500 r/min for 3 min. After the removal of incubation medium, the 4T1 cells were washed three times with PBS and then fixed by glutaraldehyde at room temperature, then rinsed with PBS and dehydrated *via* a graded ethanol series, then cleared with propylene oxide. After being embedded into EPOM812, the cell sample was then polymerized in the baking oven at 37 °C, 45 °C and 60 °C for 12 h, 12 h and 48 h, respectively. Ultrathin sections of ~70 nm thick were obtained using a diamond knife on a ultramicrotome (Leica UC6) and then transferred to a copper grid.

Detection of mitochondria membrane potential in 4T1 cells. The mitochondria membrane potential in 4T1 cells were measured by flow cytometric analysis and CLSM observation. For flow cytometric analysis, the 4T1 cells were planted into a 6-well plate (2×10^5 per well) and allowed to adhere for 24 h. Then 4T1 cells were incubated with MPR nanoparticles (400, 200, 100, 50, 25 and 0 μg/mL), MP (400 μg/mL), MPE (400 μg/mL) and MPER nanoparticles (400 μg/mL) for 24 h. At the end of incubation, the culture medium was removed and then washed for three times with PBS. After added 200 μL 0.25% trypsin for 3 min into each well of the plate, 2 mL of full culture medium was introduced to end the cell dissociation. Followed by being collected into a 15-mL centrifugal tube, the mixture was centrifuged at 1000 r/min for 5 min. Then, culture supernatant was removed and the cells precipitation was resuspended and stained with JC-1 probe (MitoScreen JC-1 kit, BD, USA). The fluorescence intensity of the cells was tested by a BD LSRFortessa flow cytometry (Becton, Dickinson and Company, USA).

For CLSM observations, 4T1 cells (10^6 cells per dish) were planted in coverglass bottom dishes (Corning Inc., New York) and allowed to adhere overnight, and then treated with MP, MPR, MPE and MPER nanoparticles at the same final concentration of 400 μg/mL. After the incubation for 24 h the media were removed, and the cells were then washed three times with PBS to remove the residual nanoparticles. The cells were treated according to Mitochondrial membrane potential assay kit with JC-1 (Beyotime Institute of Biotechnology, Shanghai, China). Red and green luminescent emissions from aggregates and monomers were excited at the wavelength of 525 nm and 488 nm, respectively.

Cell apoptosis by CCK-8 viability assays and confocal microscopic imaging. In vitro cytotoxicity of MPER nanoparticles was measured by standard CCK-8 viability assays (Cell Counting Kit, Beyotime Institute of Biotechnology, Shanghai, China) on 4T1 cells and HUVECs. In vitro cytotoxicity of MPR nanoparticles was measured by standard CCK-8 viability assays (Cell Counting Kit, Beyotime Institute of Biotechnology, Jiangsu, China) on 4T1 cells. In vitro cytotoxicity of MPE nanoparticles was measured by standard CCK-8 viability assays (Cell Counting Kit, Beyotime Institute of Biotechnology, Jiangsu, China) on 4T1 cells. Each data point was represented as mean ± standard deviation (SD) of 6 independent experiments (n = 6, n means the amount of wells in the plate for each experiment). The dose

independence of cytotoxicity was investigated at different nanoparticle concentrations.

The cytotoxicity evaluation of MPER nanoparticles on 4T1 cells was taken for an example. First of all, 4T1 cells were seeded in a 96-well plate at a density of 1×10^4 cells per well and cultured at 37 °C in 5% CO_2 for at least 12 h to allow the cells to attach. Then culture medium above was removed, then MPER nanoparticles were added into the medium, and the cells were incubated in 5% CO_2 at 37 °C for 24 h or 48 h. The concentration of MPE nanoparticles was set as 800, 400, 200, 100, 50, 25, 12.5 and 0 μg/mL. At the end of incubation, the culture medium was removed and the standard CCK-8 was used to evaluate the cell viabilities compared to the control group.

Moreover, the cell apoptosis was evaluated by the confocal microscopic imaging. The cells were divided into five groups including the control group, MP, MPR, MPE and MPER nanoparticles. After incubation for 24 h, all the cells were co-stained with calcein-AM/PI for 15 min in 5% CO_2 at 37 °C. The excess dye solution was removed and then the cells were washed three times with PBS. Subsequently, 1mL of PBS was added into the coverglass bottom dish, then the cells were taken pictures under a CLSM. Live cells and dead cells were stained with calcein-AM to present green fluorescence (λ_{ex} = 490 nm) and PI to exhibit red fluorescence (λ_{ex} = 528 nm), respectively.

Western blot analysis. 4T1 cells were divided into 5 groups including the control group, MP, MPR, MPE and MPER nanoparticles incubation. The concentrations from all of the nanoparticle groups are 400 μg/mL. After incubated for 24 h, the culture medium was removed and the cells were washed twice with 5 mL of PBS. After added 1.5 mL 0.25% trypsin for 3 min into the culture dish, 2 mL of full culture medium was introduced to end the cell dissociation. Followed by collected into a 15-mL centrifugal tube, the mixture was centrifuged at 1000 r/min for 5 min. The precipitation was measured for the Ki-67, HK2, PFK1 and PKM2 expression.

4T1 cells were divided into the control group and Fluo-4 am group and. After being incubated with Fluo-4 am for 30 min, 4T1 cells were washed with PBS for 3 times and incubated in PBS for another 30 min to ensure that fluorescence-free Fluo-4 am has turned to fluorescent Fluo-4 completely. Then, added 10 mL of full culture medium into the culture dish, and the cells were cultured for 24 h and were collected for the measurement of the glycolytic enzymes.

In vivo anticancer effect evaluation. Healthy female BALB/c nude mice (4-week-old, n = 5 in each group) were adopted for evaluation. A week later, they were transplanted with 4T1 cell (1×10^6 cells per mouse) subcutaneously. Five groups of 4T1-bearing xenografts were established to evaluate the therapeutic efficacy in vivo by intratumoral injection when the tumor volumes reached approximately 50 mm^3, including the control group (Saline), MP, MPR, MPE and MPER nanoparticles. All treatments were performed at the first, third and fifth day in the therapeutic period. Therein, the dosages of MPER nanoparticles was 25 mg/kg per time. The Control group was injected with 100 μL of saline, while the experimental groups of MP, MPR,

MPE and MPER nanoparticles dispersed in the 100 μL of saline were injected into tumor. The tumor volume ($V = (ab^2)/2$), where a and b refer to the largest length and width of tumor, respectively. After 14 days, nude mice were executed for anatomy and histopathological analyses.

Detection of Enzymes and ATP concentration in animals. At the end of the therapy, the mice were sacrificed and the tumors were collected. Then, the tumors were washed with pre-cooled PBS (0.01 M, pH 7.4) to remove residual blood. After being weighed and shredded, the tumors were ground in PBS by ball milling on ice. In order to rupture tumors completely, homogenates were then treated by sonication. Next, the homogenates were centrifuged at 5000 g for 10 minutes. The supernatants were collected for detection and quantification. The concentrations of HK2, PFK1, PKM2 and ATP were measured according to the manufacturer's instructions.

Here we take ATP detection for example. Bring all reagents and samples to room temperature before use. Then add 100 μL of each standard and sample into appropriate wells. Cover wells and incubate for 1.5 hours at room temperature. Discard the solution and wash 5 times with 1X Wash Solution. Wash by filling each well with Wash Buffer (300 μL) using a multi-channel Pipette. Complete removal of liquid at each step is essential to good performance. After the last wash, remove any remaining Wash Buffer by aspirating or decanting. Invert the plate and blot it against clean paper towels. Add 50 μL of 1x prepared Detection Antibody to each well. Cover wells and incubate for 1 hour at room temperature with gentle shaking. Discard the solution and repeat the wash procedure with 5 times. Add 50 μL of chromogenic agent A and 50 μL of chromogenic agent B to each well. After gentle shaking, incubate in the dark for 30 min at room temperature. Add 50 μL of Stop Solution in each well. Read absorbance at 450 nm in 15 min.

In vivo biodistributions of MPER nanoparticles. 15 healthy female balb/c nude mice (4 weeks) were injected with 4T1 cells (10^6 cells per mouse) subcutaneously. After the 4T1 tumors grew to 50-60 mm^3**,** the MPER nanoparticles (25 mg/kg) were injected intratumorally. Then the tumors and major organs of the mice were collected 6, 12, 24, 48 and 72 h post-injection. After these tissues rinsing with PBS (pH = 7.2), the water on their surface was removed with filter paper. After being weighed, each organ was melted by chloroazotic acid to determine the Si content by using ICP-OES.

All animal experiments in this study were performed in strict accordance with the guidelines by the Animal Care Ethics Commission of Tongji University School of Medicine (Accreditation number: SHDSYY-2018-Z0026), and the policies were approved by the Animal Care and Use Committee of Shanghai Tenth People's Hospital (Shanghai, China).

Section B: Supplementary Figures and Tables

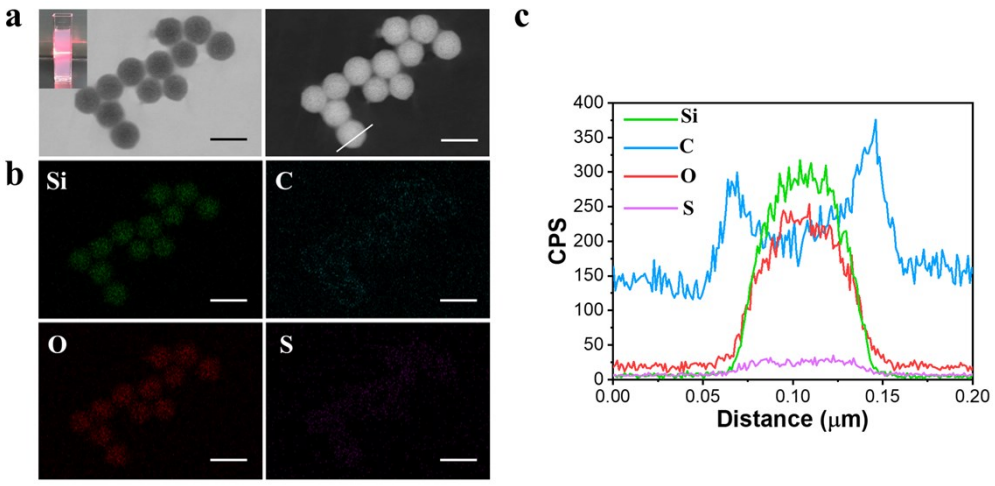

Figure S1. (**a**) STEM images of MP nanoparticles under bright (left) and dark (right) modes. Inset presents a digital photo of MP nanoparticles dispersed in the water showing Tyndall effect. Scale bar: 50 nm. (**b**) Element (Si, C, O and S) mapping images of MP nanoparticles. Scale bar: 100 nm (**c**) Line scanning profiles of MP nanoparticles. The STEM images of MP and its Tyndall effect in the water show that MP present a good dispersity in the water. The existence of C and S elements in MP nanoparticles demonstrates the success modification of PAASH on the MSN surface.

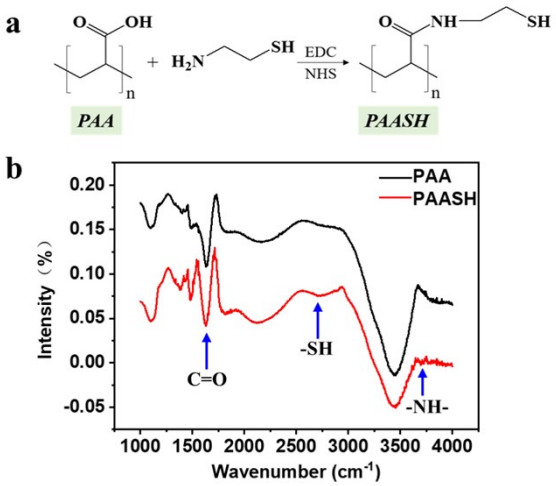

Figure S2. (**a**) Amidation reaction between PAA and cysteine hydrochloride at room temperature under the attendance of EDC and NHS. (**b**) FTIR spectra of PAA and PAASH. The adsorption band of C=O (1650 cm^{-1}) and two adsorption bands of -NH- group (3600 ~ 3900 cm^{-1}) are derived from -CO-NH-. The absorption band of -SH bonds of PAA appeared and red-shifted to 2750 cm^{-1}.

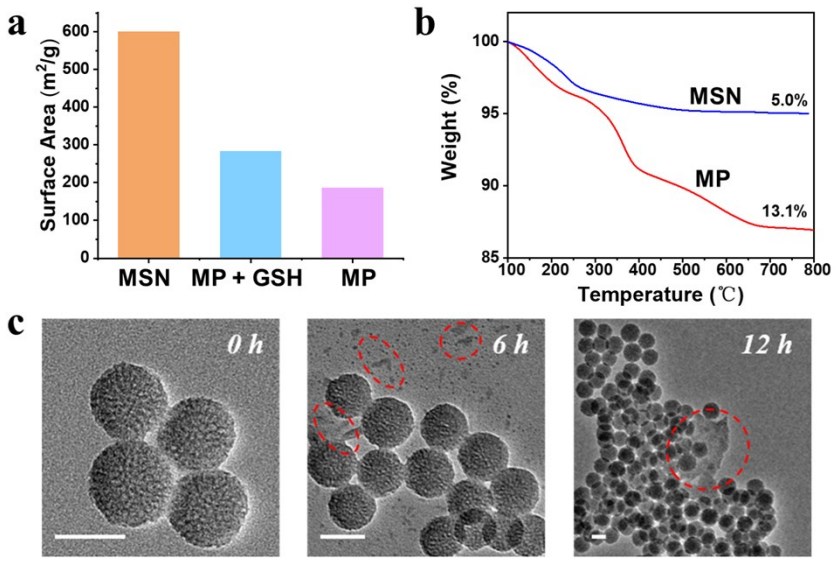

Figure S3. (**a**) Surface areas of MSN, MP exposed to GSH for 48 h and MP nanoparticles. When exposed to 10 mM GSH for 48 h, the surface area of MP nanoparticles recovered to 283.4 m^2/g. (**b**) TGA patterns of MSN and MP nanoparticles. The MP nanoparticles show a larger weight loss (13.1%) than the original MSNs (5.0%), implying that the weight percentage of the PAASH shell is about 8.1% of the MP nanoparticles. (**c**) TEM images of MP nanoparticles exposed to GSH for 0, 6 and 12 h. All of the scale bars are 50 nm. It can be found that the shells on MP nanoparticles become increasingly disrupted and even dropped off from the particle surface after reduced by 10 mM GSH for 6 and 12 h, resulted from -S-S- bond degradation in the surface layer. These results could indicate the successful modification of -S-S onto the surface of MP nanoparticles and ensure the drug release in the tumor microenvironment after endocytosed into tumor cells.

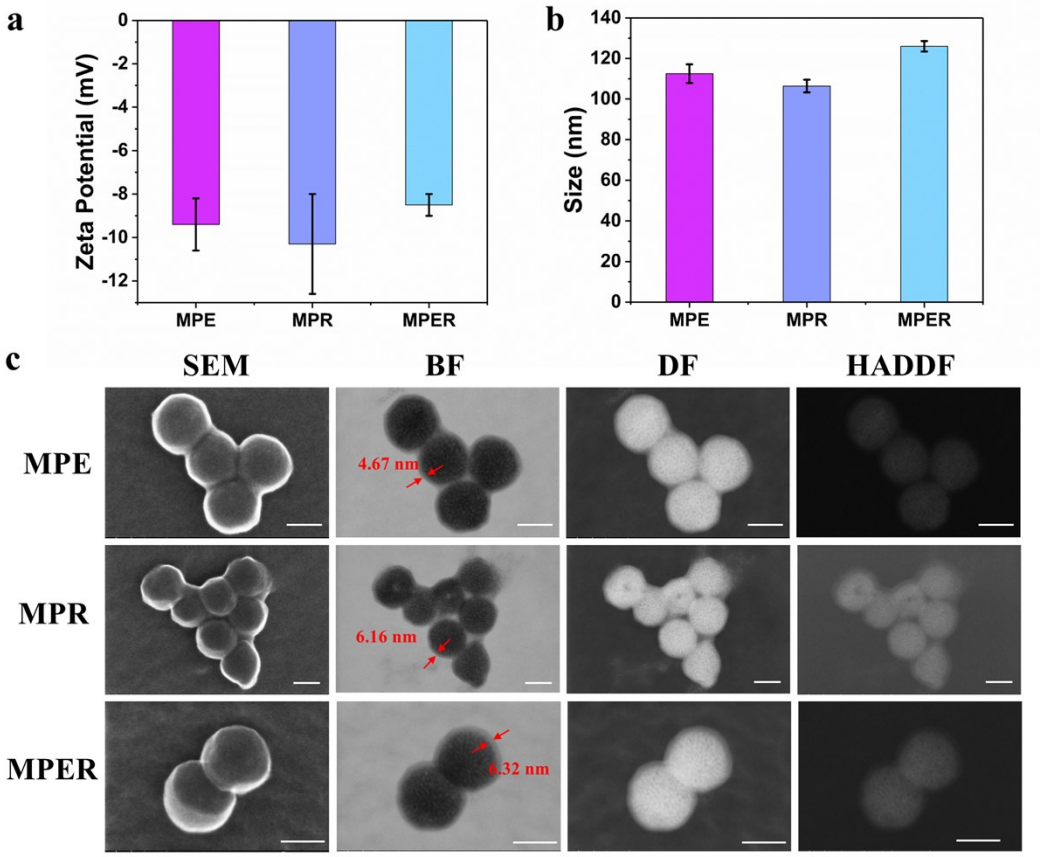

Figure S4. The characterizations of MPE, MPR and MPER nanoparticles. The zeta potentials (**a**) and DLS sizes (**b**) of MPE, MPR and MPER naoparticles. The SEM, Bright field (BF), Dark field (DF) and High-Angle Annular Dark Field (HADDF) images (**c**) of MPE, MPR and MPER nanoparticles. Scale bar: 50 nm. Due to the PAA decoration on the MSN surface, the zeta potetials of MPE, MPR and MPER nanoparticles are -9 ~ -12 mV. The DLS diameters of MPE, MPR and MPER nanoparticles are around 110 nm. It can be observed obviously that the MPE, MPR and MPER nanoparticles possess a uniform size at about 60 nm and a 4 ~ 7 nm-thick shell.

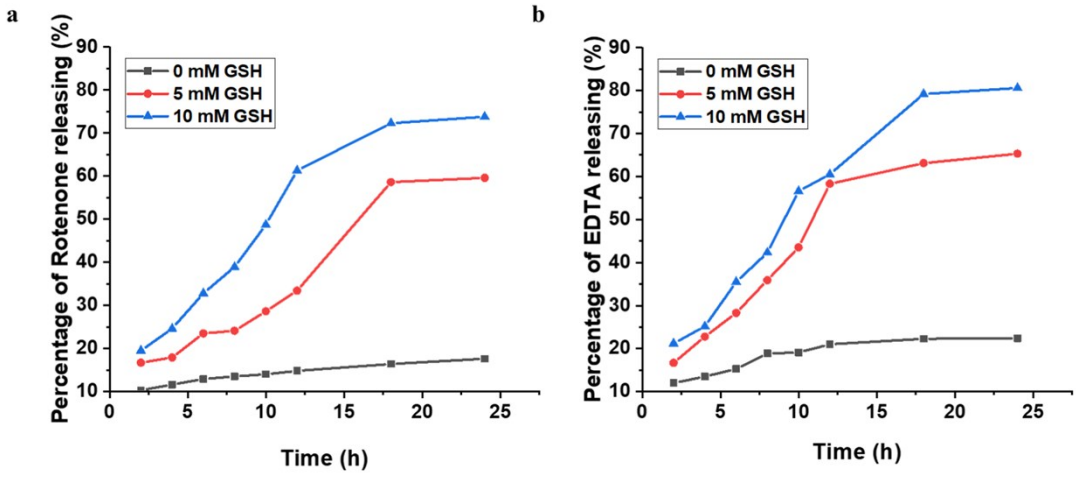

Figure S5. The releasing profiles of Rotenone (**a**) and EDTA (**b**) under different conditions. 30 mg MPER nanoparticles were sealed in a dialysis tube (3.5 kda) and dispersed in 0, 5 or 10 mM GSH buffer. Both of the Rotenone and EDTA releasing profiles were performed in a shaking table at 37 ^{o}C and at the speed of 150 rpm. The released Rotenone was measured by UV-vis. The released EDTA was detected by fluoroscent spectra after being added into Fe(III)-SSA solution. The release profiles show a relatively high releasing amount of Rotenone and EDTA in 24 h when MPER nanoparticles were exposed to 10 mM GSH than that of to 0 and 5 mM GSH.

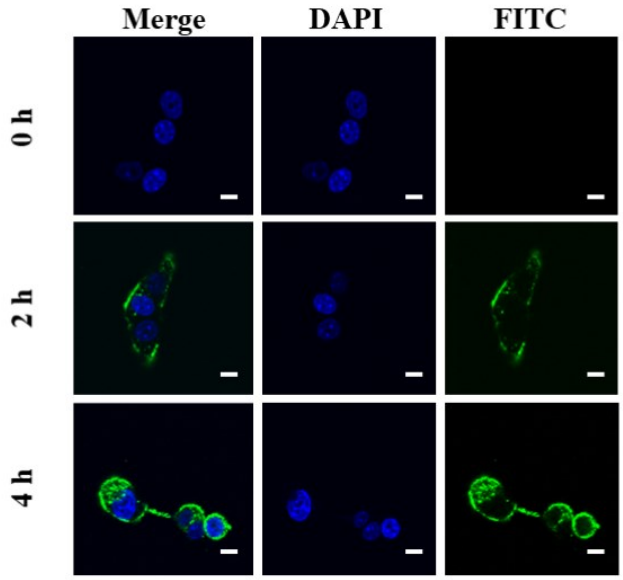

Figure S6. CLSM images of 4T1 cells incubated with FITC-labeled MP nanoparticles at the concentration of 200 μg/mL for 0, 2h and 4 h, along with the DAPI staining of nuclei. Scale bar: 10 μm. The CLSM images reveal an obvious enhancement of fluorescence intensity of the FITC-labeled MP nanoparticles in the extended incubation duration, implying the efficient intracellular uptake and ensuring the following intracellular chemical suffocation therapy for tumor cells.

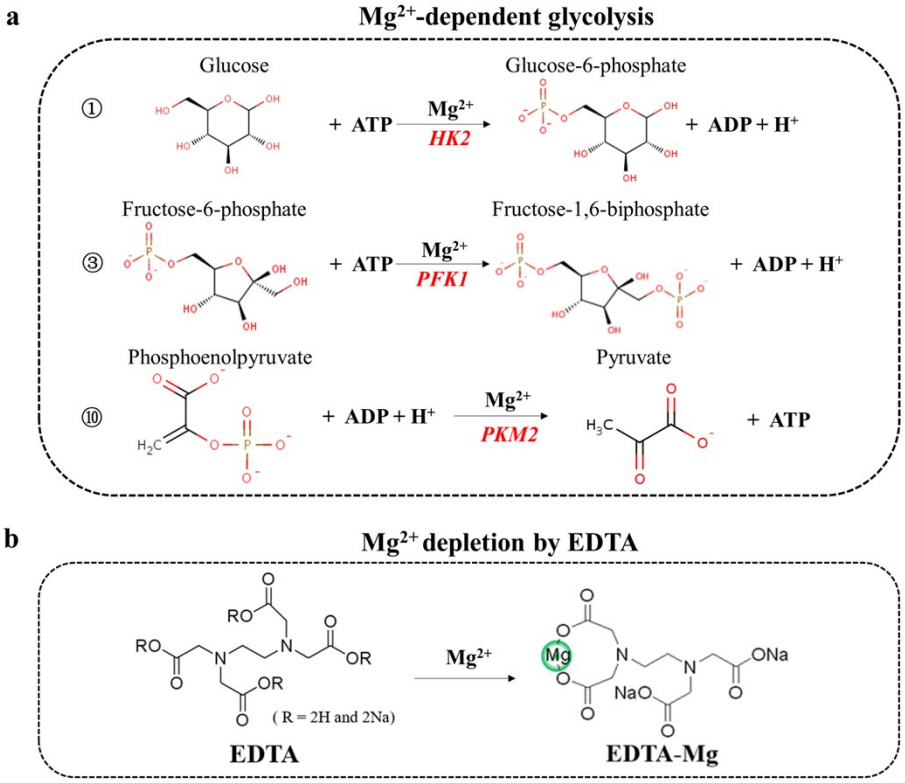

Figure S7. (**a**) The first, third and tenth reactions during the Mg^{2+}-dependent glycolytic process involved in the pyruvate generation from glucose. HK2 and Mg^{2+} could co-catalyse glucose to glucose-6-phosphate. PFK1 and Mg^{2+} could co-catalyse fructose-6-phosphate to fructose-1,6-biphosphate. PKM2 and Mg^{2+} could co-catalyse phosphoenolpyruvate to pyruvate. (**b**) The chemical equation of free Mg^{2+} in the cytoplasm depletion by EDTA.

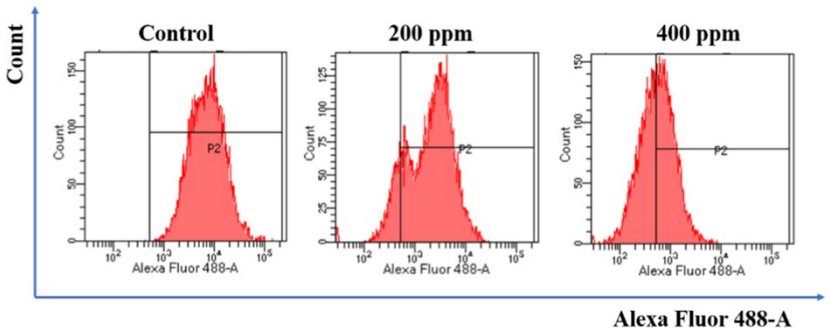

Figure S8. Flow cytometric fluorescence intensity analysis of the intracellular Ca^{2+} of 4T1 cells stained with Fluo-4 AM after being incubated with varied concentrations of MPE for 24 h. The untreated 4T1 cells were seen as the negative control. The calcium fluorescent intensity presents a remarkable fall in a MPE dosage-dependent manner.

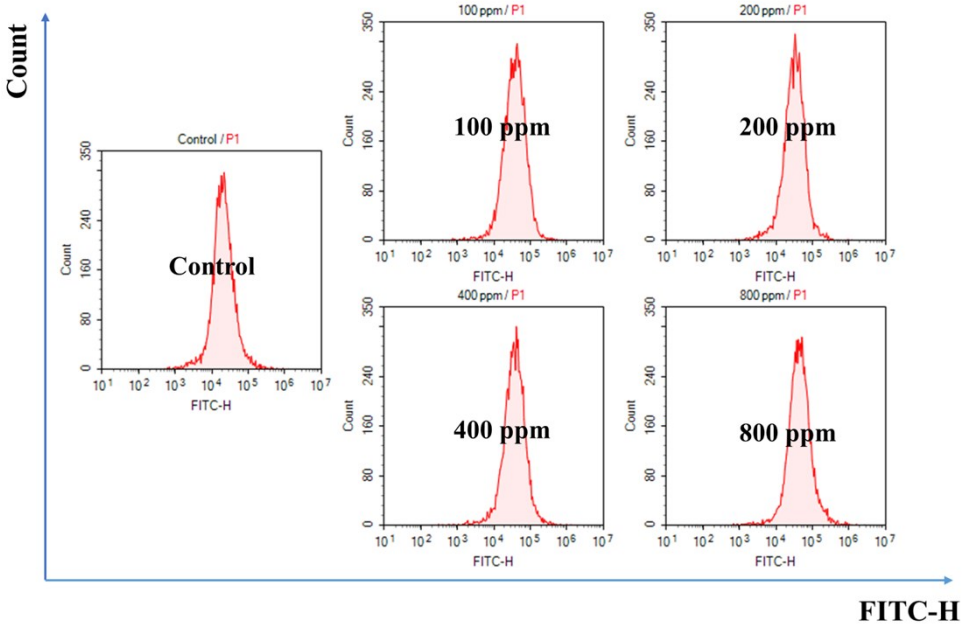

Figure S9. Flow cytometric fluorescence intensity analysis of the intracellular Mg^{2+} of HUVECs stained with Mag-Fluo-4 AM after being incubated with varied concentrations of MPE for 24 h with varied concentrations. It can be observed that the fluorescent intensity of all of the experimental groups were close to that of the control group. Even if the incubation concentration of nanoparticles was elevated up to 800 μg/mL, the fluorescent intensity of HUVECs kept almost the same to that of the control group. It can be speculated that due to the low level GSH in the HUVECs, the disulfide-decorated PAA shell would not degrade and release the contents into the cells, which ensures the biosafety of the nanoparticles.

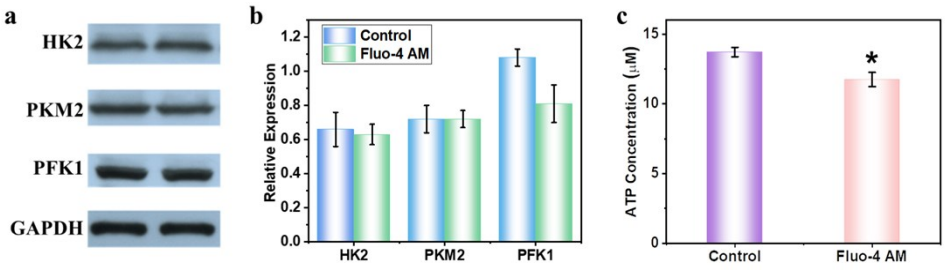

Figure S10. (**a**) Western blot analyses of HK2, PKM2 and PFK1 in 4T1 cells treated with Fluo-4 AM. (**b**) The corresponding quantifications of HK2, PKM2 and PFK1 relative expressions in 4T1 cells treated with Fluo-4 AM. All western blot data were representative of 3 independent experiments. (**c**) The ATP concentration of 4T1 cells after incubation with Fluo-4 AM. *P < 0.5. After intracellular calcium combined with Fluo-4 AM, the HK2 and PKM2 expression kept alomst the same as the untreated group, while PFK1 expression fell slightly. Moreover, the ATP concentration of 4T1 cells shows a moderate decline after Fluo-4 AM incubation.

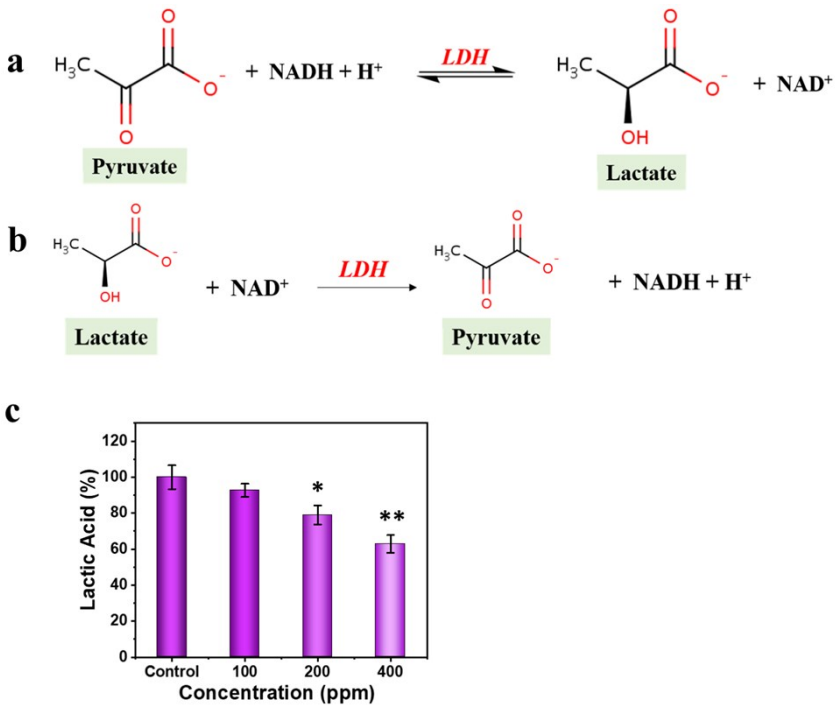

Figure S11. (**a**) After the pyruvate generation from glucose, lactate dehydrogenase (LDH) catalyzes the conversion of pyruvate to lactate. (**b**) Catalytic reaction by glycolytic enzymes of converting glucose to lactate. (**c**) Intracellular lactic acid concentration after 4T1 cells exposed to MPE nanoparticles (0, 100, 200 and 400 μg/mL) (n = 5). Statistical significance is assessed by Student's one-sided t-test compared to the control group. *$P < 0.05$, **$P < 0.01$. After incubation with MPE nanoparticles for 24 h, the intracellular lactic acid concentration shows a negative correlation with nanomaterial concentration, along with glycolytic process inhibition.

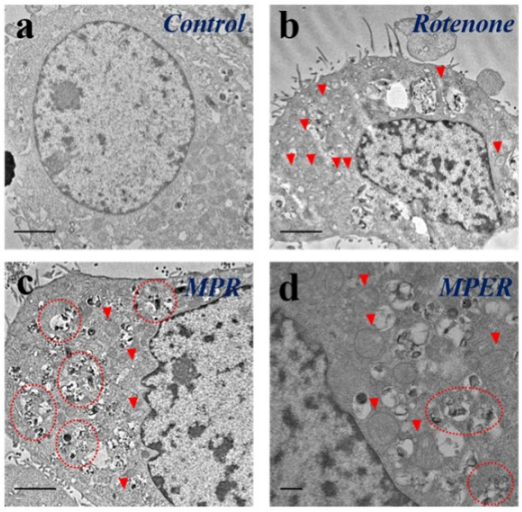

Figure S12. Bio-TEM images of 4T1 cells as the negative control, 4T1 cells treated with Rotenone as the positive control and 4T1 cells treated with MPR or MPER nanoparticles (400 μg/mL) for 24 h. As shown in the bio-TEM images, the mitochondria of untreated-4T1 cells consists of a classical double-membrane system and its inner membrane possess a specific morphology with folded cristae, while the treatment with free Rotenone led to the damaged mitochondrial inner membrane structure and an expanded matrix space. Upon the endocytosis into the cytoplasm, MPR nanoparticles released Rotenone from their pore channels, leading to the similar mitochondrial morphological changes to that of the free Rotenone group.

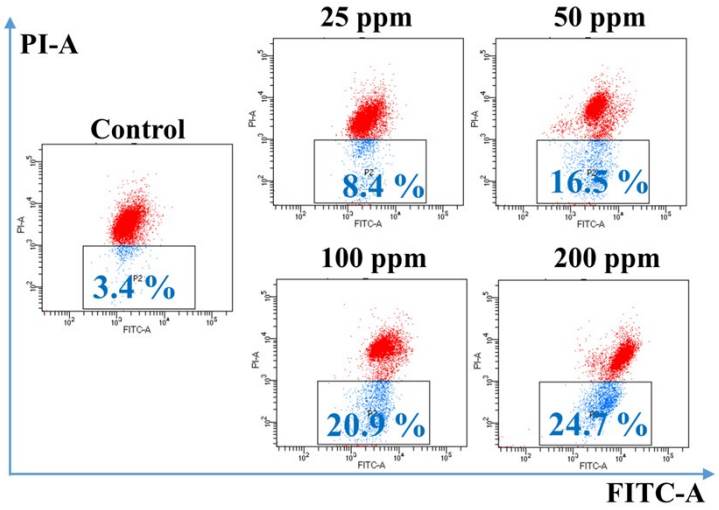

Figure S13. Flow cytometric analysis of 4T1 cells as the negative control and 4T1 cells treated with MPR nanoparticles at varied concentrations for 24 h after staining with the probe JC-1. After being incubated with MPR nanoparticles for 24 h at different concentrations, 4T1 cells were stained with JC-1 probe and their mitochondrial membrane potential variations were assessed *via* flow cytometric analysis. The dissipation of the mitochondrial membrane potential indicates the opening of the mitochondrial permeability pores, which generally defines early but irreversible stage of apoptosis. According to the difference in fluorescent intensity, cell populations are divided into two parts including live and early apoptotic cells. The flow cytometric results demonstrate a substantial enhancement of early apoptotic rate at increased MPR concentration, suggesting that the electron transport chain has been interrupted by leaked Rotenone from MPR nanoparticles.

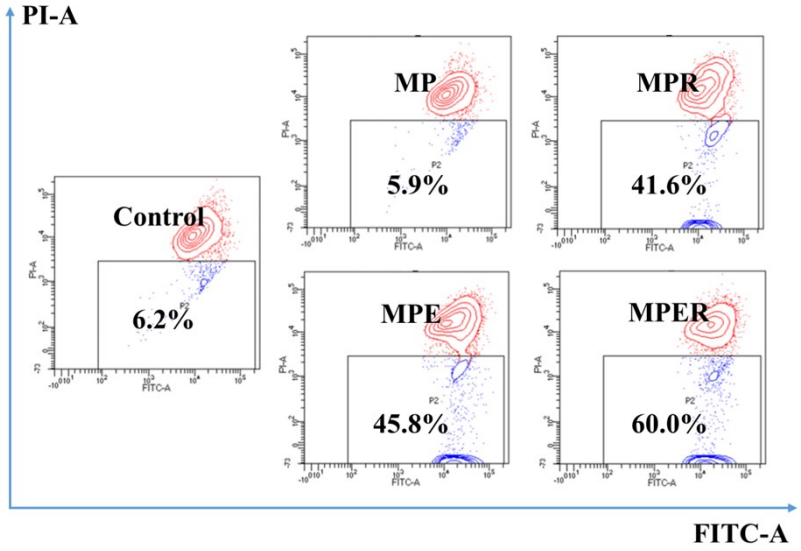

Figure S14. Flow cytometric analysis of 4T1 cells as the negative control and 4T1 cells treated with MP, MPR, MPE and MPER nanoparticles (all of their concentrations were 400 μg/mL) for 24 h and then stained with the probe JC-1. This result implies that MP nanoparticles as a drug carrier are bio-safe. Among MPE, MPR and MPER groups, MPER nanoparticle-treated 4T1 cells emit the strongest green fluorescence, suggesting the highest level of mitochondrial membrane collapse.

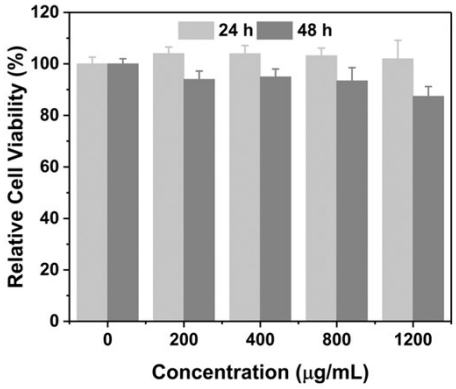

Figure S15. The relative cell viability of MP nanoparticles. The relative cell viabilities of MP-treated 4t1 cells for 24 h and 48 h with different dosages at 0, 200, 400, 800 and 1200 μg/mL were measured by CCK-8 kits. The relative cell viabilities of MP-treated 4T1 cells for 24 h and 48 h were above 90%, even when the dosage of MP nanoparticles were elevated up to 1200 μg/mL. These results show that MP nanoparticles as a drug carrier is safe to 4T1 cells, suggesting the therapeutic effect comes from the released EDTA and rotenone.

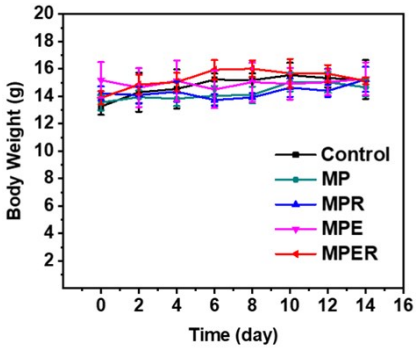

Figure S16. Time-dependent body weight curves of nude mice after different treatments. During a 14-day therapeutic period, the body weights of five groups presented neither abnormalities nor significant difference among each other.

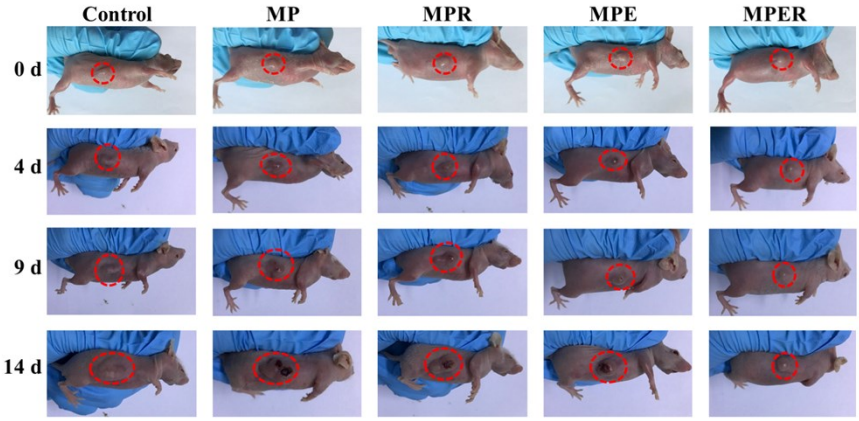

Figure S17. Digital photos of control group and four treatment groups including intertumoral injection with MP, MPR, MPE and MPER. During the therapy, tumors of MP nanoparticles group still kept growing quickly, indicating that MP nanoparticles possess no therapeutic effect in vivo. MPR and MPE nanoparticles show moderate tumor inhibition effects compared to the control group. Moreover, the tumor inhibition of MPER nanoparticles is the most remarkable.

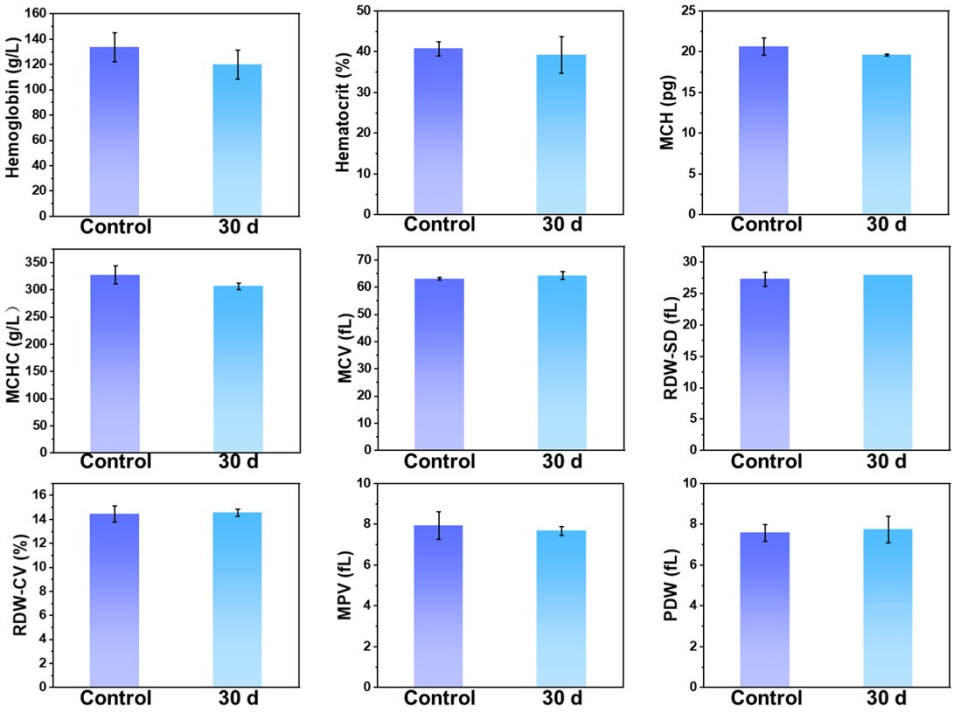

Figure S18. Hematological assay of female BALB/c nude mice. Hematological assay of mice from the control group and treatment group at MPER nanoparticles dosage of 25 mg/kg for 30 days. The blood indexes in the treatment group, including key biochemistry parameters, show no abnormality when compared to the control group.

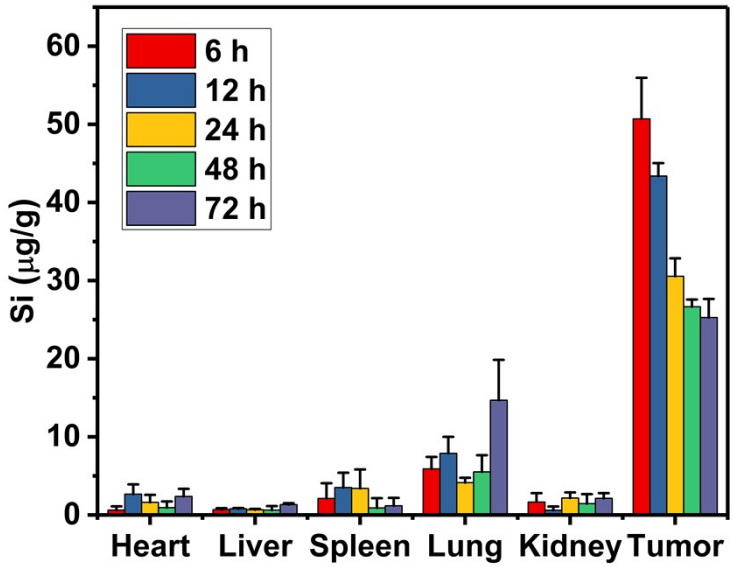

Figure S19. The in vivo Si concentrations in major organs (heart, liver, spleen, lung, kidney and tumor) after intratumoral injection of MPER nanoparticles into mice for 6, 12, 24, 48 and 72 h (n = 3). The Si concentrations were measured by inductively coupled plasma optical emission spectrometry (ICP-OES). The nanoparticles mainly accumulated in the tumors and kept at a relatively high level within 3 days. Moreover, a small amount of the nanoparticles accumulated in the spleen and lung, and few of them were in the heart, liver and kidney.

Table S1. ATP inhibition rate in 4T1 cells after being incubated with MPE or MPER nanoparticles for 24 h (n = 3). The ATP inhibition of the control group (non-treatment) is defined as 0 %. Statistical significance is assessed by Student's one-sided t-test compared to the MPE group. *$P < 0.05$.

Concentration	MPE	MPER	P value
100 μg/mL	24.64 ± 7.13 %	48.28 ± 15.70 %	0.06
200 μg/mL	58.79 ± 13.98 %	71.10 ± 5.23 %	0.15
400 μg/mL	80.16 ± 9.32 %	99.49 ± 0.71 %	0.02

Section C: Supplementary Discussions

Characterization of MP nanoparticles. The inset in **Figure S1a** presents a digital photo of MP nanoparticles dispersed in the water with Tyndall effect, indicating their remarkable hydrophilicity and dispersity. From the energy dispersive spectroscopy (EDS) element mappings and line scanning of Si, C, O and S species in the framework of MP nanoparticles (**Figure S1b-c**), it can be seen that MSN surface has been successfully modified with PAASH and MP nanoparticles present uniform size distribution. Moreover, the prepared MP nanoparticles could be well dispersed in the water for at least a week at room temperature when statically stored in a glass bottle.

Two adsorption bands of -NH- group derived from -CO-NH- can be seen from **Figure S2a-b**; meanwhile, the absorption band of -SH bonds (with a thiol functionalization percentage of 19.8%) of PAA appeared and red-shifted to 2750 cm^{-1}. Moreover, the successful assembly of PAASH shell onto the MSN was verified by the thermogravimetric analysis (TGA) of MSNs and MP nanoparticles (**Figure S3b**). The MP nanoparticles show a larger weight loss (13.1%) than the original MSNs (5.0%), implying that the weight percentage of the PAASH shell is about 8.1% of the MP nanoparticles. From the TEM images (**Figure S3c**), it can be found that the shells on MP nanoparticles become increasingly disrupted and even dropped off from the particle surface after reduced by 10 mM GSH for 6 and 12 h, resulted from -S-S- bond degradation in the surface layer. These results could indicate the successful modification of -S-S onto the surface of MP nanoparticles and ensure the drug release in the tumor microenvironment after endocytosed into tumor cells.

The characterizations of MPE, MPR and MPER nanoparticles. The zeta potentials (Figure S4a) of MPE, MPR and MPER nanoparticles are -9.4, -10.3 and -8.5 mV, respectively, due to the successful decoration of PAA on the MSN surface. The DLS average diameters (Figure S4b) of MPE, MPR and MPER nanoparticles are 112.5, 106.4 and 126 nm, respectively. From the images of Figure S4c, it can be observed directly that 4~7 nm-thick shells have been decorated on the MSN surface, producing MPE, MPR and MPER nanoparticles.

The release profile of MPER nanoparticles. The EDTA- and Rotenone-loading efficiencies of the MPER nanoparticles, which were determined using fluorescence spectra and UV-vis, were 18.9% and 2.5%, respectively. The release profiles were obtained in **Figure S5**, which show a relatively high releasing amount of EDTA and Rotenone in 24 h when MPER nanoparticles were exposed to 10 mM GSH than that of to 0 mM GSH (**Figure S5**). This result indicates that MPER nanoparticles possess a good therapeutic efficacy in TME whereas showing a relatively low contents leakage under physiological environment.

The cellular uptake of fluorescein isothiocyanate (FITC)-labeled MP nanoparticles. The intracellular uptake of fluorescein isothiocyanate (FITC)-labeled MP nanoparticles was investigated by CLSM (**Figure S6**). It can be seen that the nanoparticles localize at the margin of the cell membrane at the second hour of

cellular uptake. When the FITC-MP nanoparticles were incubated with cells for 4 h, they retained mainly in the cytoplasm. The CLSM images reveal an obvious enhancement of fluorescence intensity of the FITC-labeled MP nanoparticles in the extended incubation duration, implying the efficient intracellular uptake and ensuring the following intracellular chemical suffocation therapy for tumor cells.

The glycolytic enzymes and ATP concentration after calcium cheation by the Fluo-4 AM. As shown in the **Figure S8**, the calcium fluorescent intensity present a remarkable fall in a MPE dosage-dependent way. Therefore, we tried to find out what the this calcium elimination by EDTA would bring about in the glycolytic process. Then we investigated the glycolytic enzymes expression and ATP variation after calcium depleted by calcium fluorescent probe Fluo-4 AM, using with flow cytometric analyses and ATP assay kit, respectively. After the calcium was chelated by a sensitive calcium fluorescent probe Fluo-4 AM,[3] the relative expressions of HK2 and PKM2 have kept almost the same to the control group, while PFK1 showed a slight decline (**Figure S8a-b**). In addition, the ATP concentration has dropped by 14.3% (**Figure S8c**). These results indicate that calcium in the cytoplasm has a slight influence on the glycolytic enzymes and ATP production. In conclusion, the magnesium chelation by EDTA plays a major role in the glycolytic enzymes and ATP suppression, rather than calcium elimination, during the MPER therapy.

The mitochondria OXPHOS suppression by MPR nanoparticles. Rotenone is an effective inhibitor of mitochondrial respiratory chain complex I, blocking the electron transport during the mitochondrial oxidative phosphorylation.[4] In order to suppress OXPHOS of cancer cells, we introduced Rotenone into MP nanoparticles to prepare MPR nanoparticles. As shown in the bio-TEM images of 3 groups (**Figure S12**), the mitochondria of untreated-4T1 cells consists of a classical double-membrane system[5] and its inner membrane possess a specific morphology with folded cristae, while the treatment with free Rotenone led to the damaged mitochondrial inner membrane structure and an expanded matrix space. Upon the endocytosis into the cytoplasm, MPR nanoparticles released Rotenone from their pore channels, leading to the similar mitochondrial morphological changes to that of the free Rotenone group. The rupture of inner mitochondrial membrane facilitates the ion concentration equilibration in between the matrix and intermembrane space of mitochondria, which diminishes the H^+ gradient across the inner membrane, leading to the mitochondrial inner transmembrane potential collapses.[6] JC-1 fluorescent probe is a potential-dependent, J-aggregate-forming and delocalized lipophilic cation, often used to monitor mitochondrial membrane potential.[7] After being incubated with MPR nanoparticles for 24 h at different concentrations, 4T1 cells were stained with JC-1 probe and their mitochondrial membrane potential variations were assessed *via* flow cytometric analysis. The dissipation of the mitochondrial membrane potential indicates the opening of the mitochondrial permeability pores, which generally defines early but irreversible stage of apoptosis [8]. According to the difference in fluorescent intensity, cell populations are divided into two parts including live and early apoptotic cells. The flow cytometric results (**Figure S13**) demonstrate a substantial enhancement of early apoptotic rate at increased MPR

concentration, suggesting that the electron transport chain has been interrupted by leaked Rotenone from MPR nanoparticles.

The apoptosis of 4T1 cells detected by flow cytometry using JC-1 probe after being incubated with MP, MPR, MPE and MPER nanoparticles. The contour plots shown in **Figure S14** suggest that the fluorescence in the red zone of normally high mitochondrial membrane potentials has shifted to the blue zone (P2) of lowered mitochondrial membrane potentials. The percentage (5.9%) of low mitochondrial membrane potentials in MP nanoparticles was close to that of the control group (6.2%), which implied the biosafety of MP nanoparticles. The percentage (60.0%) of low mitochondrial membrane potentials in MPER nanoparticle-treated cells is significantly higher than those of MPR (41.6%) and MPE (45.8%) nanoparticle-treated cells, indicating the combined damaging effect of EDTA and Rotenone on mitochondria.

As shown in the **Table S1**, The ATP inhibition rate in 4T1 cells of MPER nanoparticles is significantly higher than that of MPE nanoparticles towards 4T1 cells ($^{*}P < 0.05$), proving the excellent inhibition effect of MPER nanoparticles.

In vivo biocompatibility of MPER nanoparticles. Furthermore, The blood indexes in the treatment group, including key biochemistry parameters, show no abnormality when compared to the control group (**Figure S18**). These results indicate the acceptable biocompatibility and therapeutic biosafety of MPER nanoparticles.

In vivo biodistributions of MPER nanoparticles. The tumors and major organs of the mice were collected 6, 12, 24, 48 and 72 h post-injection to determine Si content in the tumor and each organ by using ICP-OES. The nanoparticles mainly accumulated in the tumors and kept at a relatively high level within 3 days. Moreover, a small amount of the nanoparticles accumulated in the spleen and lung, and few of them accumulated in the heart, liver and kidney.

References

1. L. Pan, J. Liu, Q. He and J. Shi, *Adv. Mater.,* 2014, **26**, 6742.
2. Y. Liu, Y. Tian, Y. Tian, Y. Wang and W. Yang, *Adv. Mater.,* 2015, **27**, 7156.
3. J. Zhang, Y. Wang, Y. Zhou and Q. He, *Oncotarget,* 2017, **8**, 91223.
4. N. Li, K. Ragheb, G. Lawler, J. Sturgist, B. Rajwa, J. A. Melendez and J. P. Robinson, *J. Biol. Chem.,* 2003, **278**, 8516.
5. C. L. Hoppel, B. Tandler, H. Fujioka and A. Riva, *Int. J. Biochem. Cell Biol.,* 2009, **41**, 1949.
6. P. Marchetti, M. Castedo, S. A. Susin, N. Zamzami, T. Hirsch, A. Macho, A. Haeffner, F. Hirsch, M. Geuskens and G. Kroemer, *J. Exp. Med.,* 1996, **184**, 1155.
7. S. T. Smiley, M. Reers, C. Mottolahartshorn, M. Lin, A. Chen, T. W. Smith, G. D. Steele and L. Chen, *Proc. Natl. Acad. Sci. U. S. A.,* 1991, **88**, 3671.
8. I. Marzo, C. Brenner, N. Zamzami, S. A. Susin, G. Beutner, D. Brdiczka, R. Remy, Z. Xie, J. C. Reed and G. Kroemer, *J. Exp. Med.,* 1998, **187**, 1261.